IJCSE International Journal of Computer Sciences and Engineering Open Access
Research Paper Volume-6, Issue-1 E-ISSN: 2347-2693

Agriculture Crop Area mapping in images acquired using Low Altitude Remote Sensing

Ramesh K.N[1*], Meenavathi M.B[2]

[1*]Dept.of Electronics and Instrumentation Engineering, Bangalore Institute of Technology, Bangalore, India
[2]Dept.of Electronics and Instrumentation Engineering, Bangalore Institute of Technology, Bangalore, India

[*]*Corresponding Author: rkestur@gmail.com, Tel.: 9880642856*

Available online at: www.ijcseonline.org

Received: 12/Dec/2017, Revised: 26/Jan/2017, Accepted: 17/Jan/2018, Published: 31/Jan/2018

***Abstract*—** Ongoing research on Unmanned Aerial Vehicles (UAVs) is aimed at determining the utility of UAVs for agricultural remote sensing applications. Aerial photography from unmanned aerial vehicles bridges the gap between ground-based observations and remotely sensed imagery from aerial and satellite platforms. In the present study, Crop area measurements are carried out by analysis of aerial imagery acquired through Low Altitude Remote Sensing (LARS) carried out using a Quadcopter UAV. The area per pixel or the Ground Separation Distance (GSD) is computed using the altitude measurements from a barometer. Image processing clustering techniques are applied to classify non crop and crop area in the image extent. Further the physical crop area and non crop area is determined using GSD. In this study K-Means and Mean shift clustering techniques are used to classify crop and non crop area. Performance of determining crop area is compared for K-means and Mean shift techniques. The results indicate crop area classification using Meanshift outperforms classification using K-means.

Keywords— Unmanned Aerial Vehicle, Low Altitude Remote Sensing, Crop Area Mapping, Image clustering

I. INTRODUCTION

Unmanned Aerial Vehicles (UAVs) are unpiloted, autonomous unmanned air-crafts that can be remotely controlled or autonomously flown based on pre-programmed flight plans or more complex dynamic automation systems. The progress of this last decade in aviation technologies, miniaturization, telecommunication, automatics and embedded processing, allow UAVs to be financially accessible for the civilian world which was otherwise primarily focused on military applications.

UAVs have shown promising applications in remote sensing data collection. Unlike satellite based remote sensing systems UAVs have high spatial and temporal resolutions and can operate below cloud covers. Aerial photography from UAV bridges the gap between ground-based observations and remotely sensed imagery from satellite platforms. UAVs have successfully introduced the smaller, cheaper to operate platform paradigm among the remote-sensing community[1].

UAVs have several advantages which are useful for Agriculture remote sensing, they can operate unnoticed and below cloud covers, they can be deployed quickly and repeatedly, they are less costly and safer than piloted aircraft, they are flexible in terms of flying height and timing of missions and they can obtain very high resolution imagery. UAV sourced imagery allows for observation of individual plants, patches, gaps and patterns over the landscapes that have not previously been possible. Technological advancements of UAVs lead to development of a new concept of remote image acquisition system named Low-Altitude Remote Sensing (LARS)[2]. LARS is typically a small UAV with capabilities such as low altitude, low payload and short endurance. A LARS system is monitored by an individual having knowledge of flying a UAV. Moreover, the system can be easily assembled with off the shelf components with low repair and maintenance costs. Factors like Payload size and weight play a critical role in Agricultural LARS.

Agricultural farms in developing countries such as India and Africa are characterized by low level technology in small fragmented land holdings, mixed or diversified cropping, without capitals for bigger investments and devoid of professionally skilled workers[2]. Furthermore, rain-fed agriculture is predominately practiced (around 80% area) in the developing countries, further restricting the applicability of satellite-based remote sensing for overcast seasoned-crops. To overcome this limitation, LARS has become a promising technique and provides a highly preferred solution for the farmers. Usage of LARS technique benefits the potential users like small to medium farmers growing cash

crops such as tomatoes, potatoes and onions. The need for such simple, real-time image acquisition system substitutes the satellite-based and manned aircraft based remote sensing.

Crop area measurements provide vital inputs in farming. It provides details on the area of the crop which helps as inputs in crop planning, determining the efficiency, estimation of yield etc. LARS provides an interesting option for crop area measurement at a sub decimeter level spatial resolution which provide finer discrimination of crop area as compared to satellite based systems. Measurement of altitude is required in area computation to determine the Ground Sampling Distance (GSD). GSD can be determined either through a GPS or by using a Barometer. Nominal SPS resolution is with an error of +/- 15 metres. Differential GPS provides finer resolution upto 15 metres. However they are costly for LARS applications. Barometric altitude measurements provide an interesting cost effective option.

In this work we compute the actual crop area in an image extant of a tomato crop image acquired using LARS. The altitude measurements to compute the GSD is realized using a barometer. Clustering is carried out using K-means and Expectation maximization (EM) algorithms to discriminate crop area and non crop area. Further, GSD is used to determine the actual cropped and non cropped area in the clustered output. The crop area was analyzed for five different images acquired at different altitudes to validate the robustness of the proposed method. The performance of determining crop area is compared with EM and K-means clustering.

Rest of the paper is organized as follows. Related work is discussed in section II. The methodology is discussed in section III. The results and discussion are explained in section IV and section V concludes the research work with future scope and directions.

II. RELATED WORK

There is considerable research interest in application of LARS for agriculture LARS is find interesting applications in agriculture. Reference [3] performed imaging of a 1500 hectare coffee plantation in Hawaii. In order to conduct the test NASAs solar powered path finder plus UAV was used. The color images were useful for mapping invasive weed outbreaks and for revealing irrigation and fertilization anomalies. Miniaturization and cost reduction of electronics and hardware have enabled the use of off-the-shelf commercial UAVs. Reference [4] used a Vertical Take-off and Landing (VTOL) micro drone quad rotor aircraft to determine Leaf Area Index and Canopy cover mapping of a commercial Onion crop in 4.75 hectare commercial onion plot in Spain. Reference [5] used helicopter based UAV with hyper spectral and narrow band multispectral imaging sensors to estimate Biophysical parameters using vegetation indices of peach, corn and olive orchards. Reference [6] used a small low cost and flexible UAV with a take-off weight of 2kg and a payload of less than 500 grams to calculate Vegetation Index from visible and near Infrared images for vegetation observation in Hiroshima, Japan. Reference[7] used a fixed wing UAV with a 5.8kgs take off weight to acquire high resolution thermal imagery, to assess the variability in the water status of five fruit tree species within a commercial orchard. The assessment led to the identification of water-stressed areas and to the definition of Crop Water Stress Indices. Reference [8] used a radio-controlled unmanned helicopter-based (LARS) platform for rice crop monitoring of experimental treatment plots of 10 m x 10 m. Total biomass of rice was estimated using LARS image based Normalized Difference Vegetation Index (NDVI) values [9].

III. METHODOLOGY

Determining crop area comprises of the following steps: Image acquisition, altitude measurements and computing area per pixel and determination of total crop area under the image extent.

3.1 Study Area

The experiment site is Mudimadagu village (Latitude 13.56N, Longitude 78.36E) in Rayalpad subdivision of Srinivaspur Taluk, Kolar district, in the south west of peninsular India

3.2 Image Acquisition

Image acquisition is performed using a Raspberry Pi along with a camera module. A Linux shell script invokes the camera module and stores the aerial image every 10 seconds. Flow chart of image acquisition is shown in Figure 1

3.3 Altitude Measurements

Altitude information is required at the instant of time image is acquired, to determine the altitude at which the image was acquired. This is achieved by appending the time stamp to the name of the image while storing the image. A delay of 10 seconds was provided between every image acquisition, otherwise the system would time out and hang since concurrent USB serial port processing of altitude data was also in process. The delay of 10 seconds was experimentally determined. Minicom serial communication software tool is used to interface Raspberry PI with Arduino board. The barometric sensor is configured in Arduino programming language.

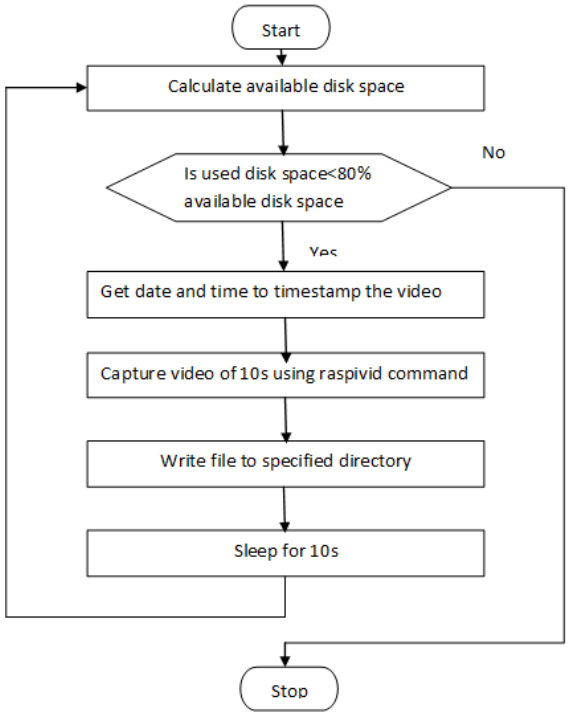

Figure 1. Image capture steps

3.4 Determination of Image Crop Area

Determination of Image crop area comprises the steps of determining the area per pixel and segmentation of cropped area and hence determining the cropped area in the image.

3.4.1 Determination of area per pixel

To determine the physical area per pixel. It is required to know the altitude of the camera at the instant the image was acquired. The barometer however continuously outputs the altitude at an average rate of 8 samples per second. To achieve time synchronization, time stamp is appended to the image filename in the linux script that captures the images. The altitude corresponding to time in the image is selected to determine the altitude of the image. An average of all the barometer readings at instant of time the image was acquired is taken for the altitude of the image. Illustrative example of determining Actual Altitude: Image filename name is 'Sat Dec 21 14 18 39 UTC 2016test23.jpg'. From the log of barometer output, the altimeter readings at [2016-12-21 14:18:39] are listed in Table 1.

Mean Altitude of Barometer measurement = 815.385 metres. The mean reference ground level = 797.33 metres Actual Altitude = 815.385 -797.334 = 18.051 metres. The Actual altitude is used to compute the area per pixel. The geometry used is HFOV = Camera Horizontal FOV, in degrees. VFOV = Camera Vertical FOV, in degrees. A = Actual Altitude in metres.

The width of the image W is given by

$$W = 2\left[\tan\left(\frac{HFOV}{2}\right) * A\right] \quad (1)$$

Similarly the height of the image is given by

$$H = 2\left[\tan\left(\frac{VFOV}{2}\right) * A\right] \quad (2)$$

The total area of the image extent is given by

$$A_t = \frac{H * W}{n_r * n_c} \quad (3)$$

Table 1. Altimeter readings

Altimeter readings	
	815.37
	815.1
	815.1
	815.1
	816.36
	815.28
Mean Altitude	815.385
stdev of altitude	0.4482466
Mean reference ground level	797.334
Actual height in metres	18.051

where n_r = no of rows in image and n_c= No of columns in the image. The image geometry is pictorially represented in Figure 2.

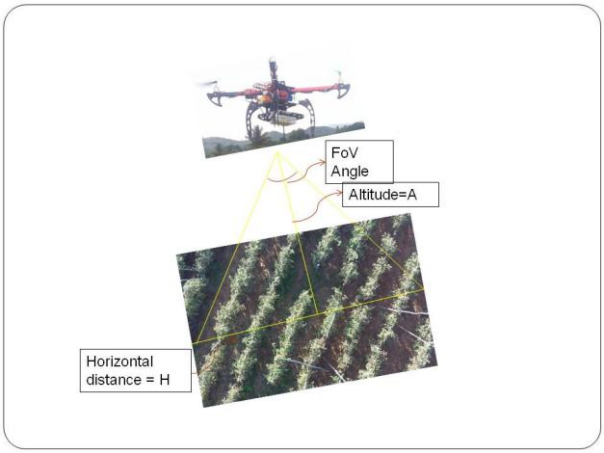

Figure 2. Image geometry

In the area computation, the altimeter reading is considered to be the vertical normal height to ground since a two axis gimbal stabilizer ensures the camera plane parallel to the ground plane.

3.5 Image processing steps

Image processing steps are shown in Figure 3, comprises the following steps .

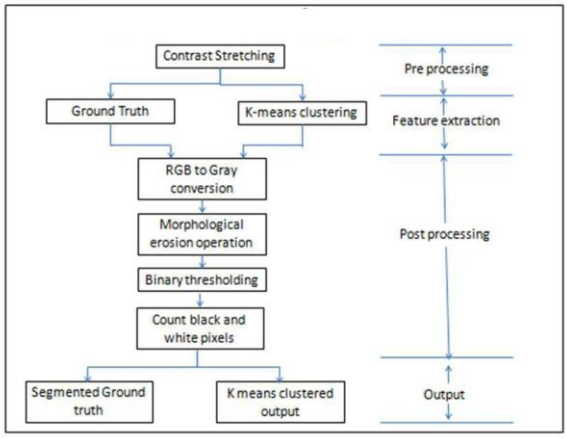

Figure 3. Image processing steps

- Contrast stretching.
- Creation of ground truth.
- Determine cropped area pixels in ground truth.
- Clustering.
  - K-means
  - Meanshift
- Determine cropped area pixels from K-means segmented image and Meanshift clustered image

Contrast stretching.

Contrast stretching of the image to eliminate intensity variation. Use of the GIMBAL stabilizer during video capture reduces the over head of image correction and alignment. Contrast stretching is required to correct the intensity chromatic errors. The image is first converted from an RGB to a CIE La*b* image. To increase the contrast, pixels at low and high intensities are saturated to their respected lower and high levels. The bottom 1% and top 1% of the pixels are saturated to increase the contrast. The image is then converted back from La*b* to RGB image

Creation of ground truth

The contrast stretched image is used in the creation of ground truth. Graphics an Image Manipulation (GIMP) tool is used to manually inspect and identify the non cropped area. The identified non-crop area pixels are marked black. The ground truth in this experiment is a pseudo ground truth since it is not possible to measure the physical area of crops under the image.

Creation of cropped area pixels in ground truth

In this step, the contrast stretched ground truth image is converted into a gray scale image. The grayscale image is converted to binary with a threshold of 0.2. Morphological operation of erosion is performed to reduce the insignificant white pixels that are not actual crop area pixels. A disk type structural element of radius 2 is used for the erosion operation. The black and white pixels are counted to determine the cropped area and non cropped area. White pixels are the cropped area and the black pixels are non cropped area.

Clustering

Crop area and non crop area is classified using clustering techniques. Kmeans [10] and Meanshift clustering [11] methods are used for comparison and validation of clustering results. The objective is two way classification and the spectral variations within the two classification is not very significant hence the simple clustering algorithms -Kmeans and Mean shift are used. C++ programming using OpenCV C++ libraries in Microsoft Visual C++ environment is used to realise K-means and Meanshift algorithms. The pre and post processing of images is performed using MATLAB technical computing software.

Kmeans clustering: K-means is a simple and well known non parametric unsupervised clustering algorithm. Spectral values of the image is the dataset. The number of clusters K is defined apriori. In this experiment the number of clusters were determined empirically and set to 4. Although it is a two cluster classification, the k value was set to 4 to account for the granularity of thresholding in the subsequent stage. The max iterations was set to 100. K-means algorithm steps are

Start:

Step 1: Initialize the centroids c_j with random numbers in the range 0 to 255, where j= 1,2,...k

Step 2: For every x_i= 1 For c_j = 1,2,....,k where i= 1,2,....n compute the Euclidian distance

$$d(x_i, c_j) = \sqrt{(x_2 - x_1)^2 + (y_2 - y_1)^2 + (z_2 - z_1)^2} \quad (4)$$

where x_2,y_2,z_2 are the spectral coordinates of x_i and x_1,y_1 and z_1 are the co-ordinates of the centroid c_j

group x_i to min of c_j

Step 3: Repeat Step 2 for all x_i

Compute the new mean c_j'. c_j' is the mean of all x_i s mapped to the centroid c_j

Step 4:

If $c_j' \neq c_j'$ go to Step 2, else END

STOP

Meanshift clustering : Pyramid mean shift Given a set of samples $\{x_i | i = 1, 2, 3, ...n\}$ in the d-dimensional feature space, the kernel density estimator and the weight function are respectively presented by symmetric kernel function G(x) and w(x) . The mean shift vector is defined as:

$$M(x) = \frac{\sum_1^n G(x - x_i) w(x_i)(x - x_i)}{\sum_1^n G(x - x_i) w(x_i)} \quad (5)$$

The mean shift vector is aligned with the local gradient estimate which always points toward the direction of maximum increase in the density. So the point reaches at the peak of each mode of the density until the mean shift vector M(x) becomes zero. Equation (5) can be changed into the following form:

$$M(x) = \frac{\sum_1^n G(\frac{x - x_i}{h}) w(x_i)(x - x_i)}{\sum_1^n G(\frac{x - x_i}{h}) w(x_i)} \quad (6)$$

where *h* is the bandwidth. *x* is assigned to *y* and iterated until y=x. The algorithm steps are

- set starting point $x = x_0$, allowable error ζ
- Repeatedly calculate *y* using (6)
- if $\| y - x \leq \| \zeta$ is true, then quit else assign *y* to x and recompute *y*

The convergence value of each of the pixel needs to computed in every iteration hence the computational complexity is high. Gaussian pyramid are used to reduce the no of pixels for which the convergence value need to be computed. The parameters used in this experiment are levels of hierarchy of Gaussian pyramid = 2, Spatial window radius = 20 and color window radius = 40

Clustering performance evaluation

The performance of the image classification and segmentation algorithm is evaluated using Receiver Operating Characteristics (ROC) error estimation methods [12]. A two class binary classification is used. ROC is calculated for the image in terms of True Positive (TP), False Positive (FP), True Negative (TN) and False Negative (FN). A pixel which is a crop and which is positive according to the ground truth and also according to the computed result is a True Positive while a pixel which is positive according to the computed result but negative according to the ground truth is a False Positive. Similarly, a pixel which is negative according to the ground truth and also according to the computed result is a True Negative while a pixel which is negative according to the computed result but positive according to the ground truth is a False Negative. The following evaluation features derived from the confusion matrix are used. Sensitivity or True Positive Rate (TPR)

$$TPR = \frac{TP}{FP+FN} \quad (7)$$

$$TNR = \frac{TN}{TN+FP} \quad (8)$$

$$FPR = \frac{FP}{TN+FP} \quad (9)$$

$$ACC = \frac{TP+TN}{(TP+FP+TN+FN)} \quad (10)$$

$$FDR = \frac{FP}{(FP+TP)} \quad (11)$$

IV. RESULTS AND DISCUSSION

4.1 UAV flight

The images are acquired using the built UAV which is flown to a maximum altitude of 18 metres and for a flight duration of 6 minutes. The copter hovered for an area of 0.4 hectares. Altitude measurements are listed in Table 2. It can be seen from Table 2 that the standard deviation(sd) is within the range of the manufacture detailed barometer specification of .1%. For purpose of computing the mean altitude is considered as the actual altitude. Mean reference ground level = 797.33m and standard deviation = 0.519

4.2 Determining area per pixel and the total area in an image

Within a set of images captured for a flight time of 5 minutes, five images were selected which provided the complete details required for the crop area determination. The altitudes of the images are tabulated in Table 3. The altitude range of the images was from 4.9 metres to 18.05 metres. Table 3 provide the details of captured area of the images. The area covered in an image is in the range of 17.22 square metres to 232.61 square metres. The maximum area covered within the image frame is 232.61 square metres at an altitude of 18.01 metres. The resolution at this altitude was .46 millimetre per pixel

Table 2 Altitude measurements

Image no	No of samples	Mean Altitude in metres	Std Deviation	Actual Altitude in metres
I1	8	802.243	0.73	4.9
I2	7	804.97	0.59	7.63
I3	6	815.385	0.44	18.05
I4	8	813.39	0.7	16.76
I5	8	807.598	0.62	10.26

Table 3. Cropped area of image

Image No	I1	I2	I3	I4	I5
Actual Altitude, in metres	4.9	7.63	18.01	16.76	10.26
Breadth in metres	4.88	7.6	17.94	16.69	10.22
Length in metres	3.53	5.49	12.97	12.07	739
Area per pixel in square centimetres	0.000003417	0.000008285	0.000046162	0.000039977	0.000014982
Total Area in square metres	**17.22**	**41.75**	**232.61**	**201.44**	**75.49**

Image output of the image processing steps of the five images are shown in Figure 4 to Figure 8

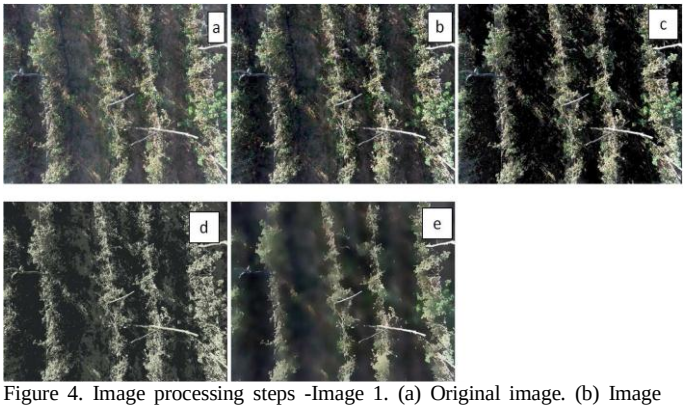

Figure 4. Image processing steps -Image 1. (a) Original image. (b) Image enhanced by contrast stretching. (c) Ground truth image.(d) Kmeans clustering. (e) Meanshift clustering

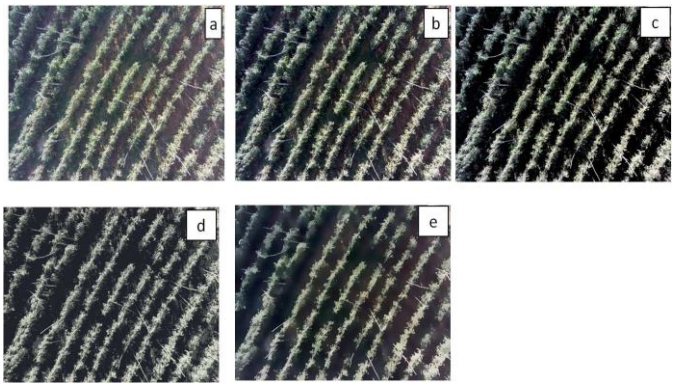

Figure 5 Image processing steps -Image 2. (a) Original image. (b) Image enhanced by contrast stretching. (c) Ground truth image.(d) Kmeans clustering. (e) Meanshift clustering

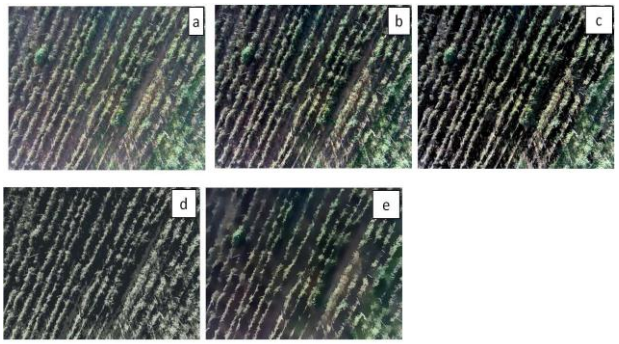

Figure 6. Image processing steps -Image 3. (a) Original image. (b) Image enhanced by contrast stretching. (c) Ground truth image.(d) Kmeans clustering. (e) Meanshift clustering

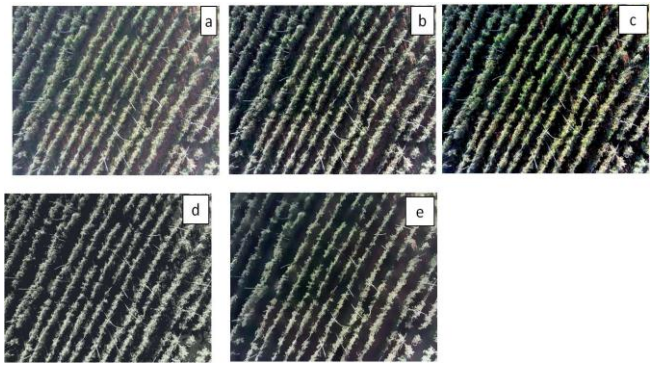

Figure 7 Image processing steps -Image 4. (a) Original image. (b) Image enhanced by contrast stretching. (c) Ground truth image.(d) Kmeans clustering. (e) Meanshift clustering

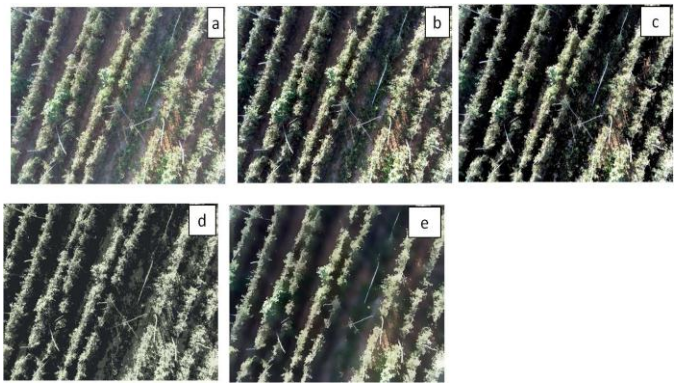

Figure 8. Image 5. (a) Original image. (b) Image enhanced by contrast stretching. (c) Ground truth image.(d) Kmeans clustering. (e) Meanshift clustering

Table 4 lists the classification of crop area and non crop area with in an image extent both in terms of the crop area pixels and the physical area of cropped area and non cropped area with in the image extent. Table 5 lists the Clustering confusion matrix for performance evaluation of clustering. The mapping to predicted and Actual class in Table 6 are

Predicted Class + = Ground truth crop pixel

Predicted class -= Ground Truth uncropped pixel
Kmeans Actual class + = Kmeans cropped pixel
Kmeans actual class -= Kmeans uncropped pixel
Meanshift Actual class + = Meanshift cropped pixel
Meanshift Actual class -= Meanshift uncropped pixel.

Table 4. Area classification

Image number	I1	I2	I3	I4	I5
Crop area pixels -ground truth	1669160	1733716	1946345	1938668	2124787
Non crop area pixels -Ground truth	3369688	3305132	3092503	3100180	2914061
Crop area pixels-Kmeans	1834935	1643705	1856950	1767623	2068273
Non Crop area pixels-Kmeans	3203913	3395143	3181898	3271225	2970575
Crop area pixels - Meanshift	1557941	1708675	1881469	1788107	2054757
Non Crop area pixels-Meanshift	3480907	3330173	3157379	3250741	2984091
Crop area in sq metres-Ground truth	5.7	14.36	89.85	77.5	31.83
Non Crop area in sq metres Ground truth	11.51	27.38	142.76	123.94	43.66
Crop area in sq metres - Kmeans	6.27	13.62	85.72	70.66	30.99
Non Crop area in sq metres -Kmeans	10.95	28.13	146.88	130.77	44.5
Crop area in sq metres - Meanshift	5.32	14.16	86.85	71.48	30.78
Non Crop area in sq metres - Meanshift	11.89	27.59	145.75	129.95	44.71

Table 5 Clustering confusion matrix

Image number	I1		I2		I3		I4		I5	
	Predicted class		Predicted class		Predicted class		Predicted class		Predicted class	
Ground truth	+	-	+	-	+	-	+	-	+	-
Kmeans Actual class +	1669160	165775	1643705		1856950		1767623		2068273	
Kmeans Actual class -	0	3203913	90011	3305132	89395	3029503	171045	3100180	56514	2914061
Meanshift Actual class +	1557941		1708675		1881469		1788107		2054757	
Meanshift Ac-tual class -	111219	3369688	25041	3330173	64876	3092503	150561	3100180	70030	2914061

Figure 9. shows the classification performance measures of 5 images with KM and MS algorithm. The FPR and FDR are plotted on secondary axis while the other measures are plotted in primary Y axis. It can be observed that MS performs better than K-means on all the parameters

Figure 9. Classification performance

V. CONCLUSION AND FUTURE SCOPE

Crop area measurement is successfully performed on tomato crop imagery acquired using LARS. LARS was carried out using a Quadrotor UAV. Five images were analyzed to validate the robustness of the proposed method. Clustering of crop area and non area crop pixels was carried out using K-means and Meanshift algorithms. Results indicate that meanshift clustering outperforms K-means algorithm. The results are promising. This work demonstrate the potential of LARS for agriculture applications in crop vegetation analysis using UAVs. The work can be extended to measure the crop area of large swaths by analysing mozaiced images.

REFERENCES

[1] Colomina .I, Molina .P, "*Unmanned aerial systems for photogrammetry and remote sensing*", A review ISPRS Journal of Photogrammetry and Remote Sensing 92, 7997 (2014)

[2] Swain Kishore Chandra, Jayasuriya, H.P.W. , " *Low Altitude Remote Sensing Applications for Diversified Farming Conditions in Developing Countries: An Overview*", AsiaPacific Journal of Rural Development. Vol. XVIII, No. 2, De¬cember 2008

[3] Herwitz S.R, Johnson L.F, Dunagan S.E, Higgins R.G, Sullivan D.V, Zheng J, Lob¬itz B.M , Leung .J, Gallmeyer B.A ,Aoyagi M, Slye R.E, Brass J.A, 2004, "*Imaging from an unmanned aerial vehicle: agricultural surveillance and decision support*", Computers and Electronics in Agriculture 44 4961, 2004

[4] Juan I. Corcoles, Jose F. Ortega, David Hernandez , Miguel A. Moreno, 2013, "*Estimation of leaf area index in onion (Allium cepa L.) using an unmanned aerial vehicle*", Biosystems Engineering 115(2013) 31-42, 2013

[5] Jose A. J. Berni, Pablo J. Zarco-Tejada, Surez Lola , and Fereres Elias, "*Thermal and Narrowband Multispectral Remote Sensing for Vegetation Monitoring From an Unmanned Aerial Vehicle*", IEEE transactions on Geoscience and Remote Sensing , vol. 47, NO. 3, march 2009

[6] Suzuki Taro, Amano Yoshiharu, Jun-ichi Takiguchi, Hashizume Takumi, Suzuki Shinji and Yamaba Atsushi, "*Development of Low-cost and Flexible Vegetation Monitoring System Using small Unmanned Aerial Vehicle*", ICROS-SICE International joint Conference, Fukuoka International Congress Center, Japan, 2009.

[7] Dugo Gonzalez .V , Zarco-Tejada .P, Nicols .E , Nortes P.A, Alarcn J.J, Intrigli¬olo D.S and Fereres .,"*Using high resolution UAV thermal imagery to assess the variability in the water status of five fruit tree species within a commercial orchard*", International Journal on Advances in Precision Agriculture, 2013

[8] Swain, Kishore C., and Qamar Uz Zaman. *"Rice crop monitoring with unmanned helicopter remote sensing images."* Remote Sensing of Biomass-Principles and Applications. InTech, 2012.

[9] Carlson Tobu N and Riziley A.David, " *On the Relation between NDVI, Fractional Vegetation Cover, and Leaf Area Index*", REMOTE SENS. ENVIRON. 62241-252 1997.

[10] Selim S.Z. and Ismail M.A. , 1984 ,"*K-means type algorithms: a generalized con-vergence theorem and characterization of local optimality*", IEEE Transactions on Pattern Analysis and Machine Intelligence 6 8187, 1984 8187

[11] Comaniciu, D. and Meer, P. "*Mean shift: A robust approach toward feature space analysis*". IEEE Transactions on pattern analysis and machine intelligence, 24(5), pp.603-619, 2002

[12] Fawcett T ,"*Roc graphs: notes and practical considerations for researchers*". Technical Report HPL-2003-4, HP Labs, 2006.

Authors Profile

Ramesh K.N received his B.E. degree in Electronics engineering from Bangalore university in 1995, the ME degree in Electronics and Communication in 2015 from University Visvesvaraya college of Engineering. Ramesh K.N has 17 years of work experience at Infosys Technologies Ltd, Bangalore. He was a Group Project Manager at Infosys. He has

worked in development of features for Core switching and Digital Centrex products in the area of communication protocol development, call processing, translations and routing software. He is currently a Ph.D student in the department of Electronics and Instrumentation at Bangalore Institute of Technology, Bangalore. His research interests include Image processing, machine learning and remote sensing from UAVs.

Dr. Meenavathi M.B. received her B.E. degree in Electronics and Communication Engineering from the Mysore university in 1989. ME. degree in Digital Techniques and Instrumentation from university of Indore, Madhya Pradesh in 1994 and Ph.D. degree in Electronics and Communication Engineering from Dr MGR university, Chennai in 2010. She is curently working as a Professor and Head of department of Electronics and Instrumentation Engineering at Bangalore Institute of Technology, Bangalore. Her research interests include Image processing, signal processing, Neural Networks and fuzzy logic.

